

Elastic and inelastic analysis of non-prismatic members using finite difference

SAMEER A. HAMOUSH^{*}, MOHAMED J. TERRO^{**},
AND W. MARK MCGINLEY^{***}

^{*}*Dept. of civil and architectural Engineering, North Carolina A&T State University, Greensboro, NC27411, USA.*

^{**}*Kuwait University*

ABSTRACT

This paper studies the elastic and inelastic behavior of non-prismatic members subjected to combined eccentric axial and transverse forces. The inelastic material behavior of the member is taken into account using a bi-elastic constitutive relationship of the stress and strains. This is to simulate the elastic and inelastic analysis as well as elastic perfect plastic analysis. This is necessary to carry the model on various materials including metals, concrete and composites. Based on the curvature-deflection relationship, a finite difference technique is implemented to simulate the deflected shape of non-prismatic members. An analytical computer model for the sectional equilibrium of the member is developed. Exact solutions for six cases of strain in the pure elastic, elastic-plastic, and pure plastic modes in both tension and compression are considered. The model relates beam curvature to deflection by analyzing strain distribution at sections of the member for a given bending moment and axial force. The presented model provides a solution for any non-prismatic beams, but the focus of this investigation is on tapered beams only. Numerical examples are presented and validated against elastic solutions.

Keywords: Axial and transverse loading; beam-column; computer model; elastic and inelastic. finite difference; non-prismatic.

1. INTRODUCTION

Beams that are deepened by haunches, to increase their moment resistance, and non-prismatic columns, such as those supporting crane girders in industrial buildings, are widely used in engineering practice. The elastic and inelastic analysis of such non-prismatic members is well documented in the literature. However, the inelastic analysis of non-prismatic members is limited to the use of finite element and equivalent systems methods. Furthermore, most of the work on equivalent systems has been established for cases where the loads are applied only in the transverse direction, and do not account for axial loads.

Ferdis (1956, 1966, 1973, and 1984), and Ferdis and Zobel (1958 and 1961)

developed the method of equivalent systems which used a double integration technique to analyze prismatic members subjected to flexure only. The predicted behavior of members under pure bending using this method compared favorably with experimental results available in the literature. Ferdis and Keene (1990) and Ferdis and Taneja (1991) further extended the equivalent systems method to cover both prismatic and non-prismatic members in the inelastic range. This method permits the replacement of the original member of variable stiffness with one of uniform equivalent stiffness. By using this technique they predicted the member behavior up to failure. Their study, however, did not include members with axial loading.

El-Mezaini *et al.* (1991) used isoparametric plane stress finite elements to conduct an investigation of the behavior of frames with non-prismatic members. Their study showed that the conventional methods of analyzing these type of structures lead to erroneous results. Therefore, they recommended the use of frame analysis computer programs to model frames which contain non-prismatic members.

Funk and Wang (1988) developed a numerical technique for the calculation of a stiffness matrix for non-prismatic members. This technique, coupled with the finite element method, was used to obtain the deflections at nodes along the member. The method, however, was not able to accurately predict the behavior of the non-prismatic members in the inelastic range. Also, Resende and Doyle (1981) and Mumuni (1983), working separately, developed finite element models for the analysis of non-prismatic beams in the elastic and inelastic range. These models are considered a reinforcement of the conventional finite element method.

This paper describes the development of a versatile and simple numerical technique to study the behavior of non-prismatic beam-column members stressed beyond their elastic limit. This technique uses a finite difference approach over the length of the member coupled with force equilibrium and strain compatibility equations applied across the section. Validation of predicted member response against results obtained using other available numerical techniques is presented.

The proposed model of this investigation was applied to reinforced concrete beams (Shahid, 1998) and beams reinforced with FRP composite materials to evaluate the deflection and the curvature along the cantilevered beams (Hamoush *et al.* 2001). It was found that the proposed model predicted the deflection with a reasonable accuracy.

2. FORMULATION

In this section, the finite difference formulation and the inelastic beam-column sectional analyses are described.

Finite difference formulation

Using a Taylor approximation for beam-column member, the finite difference relationship between curvature and deflection is presented below (Allen and Bulson 1980):

$$W_{n+1} = h^2 W''_n + 2W_n - W_{n-1} \tag{1}$$

Where:

h = length of segments along the member, W = total displacement, n = station number, and W'' = curvature.

Equation (1) provides the displacement at the end station when those at the two previous stations are known, coupled with the curvature at the previous station. It should be noted that higher order terms are neglected based on the assumption of small deflections. However, equation (1) could be easily modified to include higher order terms by using a Runge-Kutta approximation.

The curvature ($W'' = \frac{1}{\rho}$, where ρ is the radius of curvature) is determined assuming a linear strain distribution across the section at each station. This linear strain distribution is defined by a top and bottom value of strain at each end of the section. The top and bottom strains are calculated based on the equations of equilibrium of the applied forces and the compatibility of strains at each section. The boundary conditions for equation (1) are dependent on the types of support used for the member under consideration.

(a) Simply supported ends

For beam-columns with simply supported ends, there are zero displacements at both ends (see Figure 1).

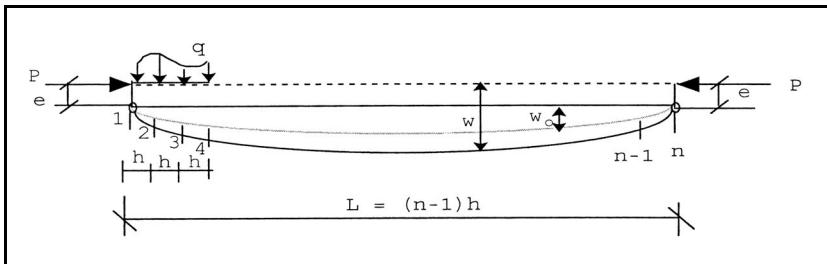


Figure 1: Finite difference modeling of a simply supported beam.

Where:

W_0 = initial displacement of unloaded member measured from the line joining the ends of the center-line, e = eccentricity of the compressive load, and P = applied load.

To apply the finite difference approach, a value for the displacement at station 2 must be assumed. Based on this value, the applied moment and axial force are determined. Strain compatibility relations are then employed to calculate the top and bottom strain values and the curvature of the section as shown in the following sections. Having initial values for displacement at stations 1 and 2 (displacement at station 1 equals zero), equation (1) is then used to determine the displacement at station 3. The displacement at station 4 is then calculated knowing the values at stations 2 and 3. This process is continued along the member until the station at the end support is reached. If the end displacement coincides with the actual support conditions, i.e. zero displacement, then the assumed initial deflection at station 2 represents a true solution. Otherwise, a new assumption is made based on the difference between the calculated and the actual end conditions.

It should be noted that the applied moment at any station includes bending due to the transverse loading in addition to the moment generated by the applied eccentric load P . The method, therefore, accounts for geometric nonlinearities by considering the $P - \delta$ effect. Furthermore, since the deflections are measured from the center lines, initially curved members can also be accounted for by this method.

(b) Fixed-end supports

In cases where the ends of the beam-column member are fixed, zero values for both the end displacements and rotations are imposed. To satisfy these boundary conditions, an analysis is first conducted with the end displacement set to zero, as described for the case of a simply supported beam-column. This analysis will yield a set of displacement values at stations along the member. To obtain zero end rotations, a fixed-end moment is applied at each end of the beam based on the value of displacement at the stations adjacent to the ends. This fixed-end moment is calculated as follows:

If W_n represents the displacement at the end, an imaginary station $n + 1$ is assumed with the following displacement value:

$$W_{n+1} = h^2 W_n'' + 2W_n - W_{n-1} \quad (2)$$

But the rotation at station n equals zero ($\frac{dw}{dx} = 0$) which can be numerically formulated as:

$$\frac{W_{n+1} - W_{n-1}}{2h} = 0 \quad (3)$$

Therefore,

$$W_{n+1} = W_{n-1}$$

Substituting equation (3) into equation (1) leads to the curvature at the end:

$$W_n'' = \frac{2(W_{n-1} - W_n)}{h^2} \quad (4)$$

Using the values of the curvature at station n and the constant axial load P , the top and bottom strain values are calculated. The fixed-end moment is then easily determined based on these strain values using the procedures described in the later sections.

A second simple-end analysis is then carried-out with the calculated fixed-end moment added to the applied loads. A new set of deflection values are then obtained along the member leading to an incremental fixed-end moment which is added in turn to the previous loads. The analysis is continued until the incremental moment becomes within the tolerance.

(c) Simple and fixed-end supports

In cases where the beam-column is fixed at one end and simply supported at the other, end displacements at the two supports and one end rotation are restrained. The solution will be accomplished by performing an analysis with simple supports first, followed by a second one with an imaginary station extended beyond the fixed-end location to ensure zero rotation. The calculated fixed-end moment is then added to the loads at the fixed end and the analysis is continued until convergence in a fashion similar to that of two fixed ends discussed in the previous section.

Inelastic Behavior of Beam-Columns

The inelastic analysis in the proposed model is based on the assumption that plane sections remain plane during loading. Under applied loading, the unit elongation of a fiber at distance y from the neutral surface is described by Timoshenko (1969 and 1976) and shown below:

$$\varepsilon = \frac{y}{\rho} + \varepsilon_0 \quad (5)$$

Where, ε_0 is the strain shifting from pure bending caused by the axial force; the distance of the neutral axis from the upper surface is denoted by $h_1 = \varepsilon_1 \rho$. and the distance between the neutral axis and the lower surface is $h_2 = -\rho \varepsilon_2$, where ρ is the radius of curvature.

The magnitude of the applied compressive force is given in the following relation:

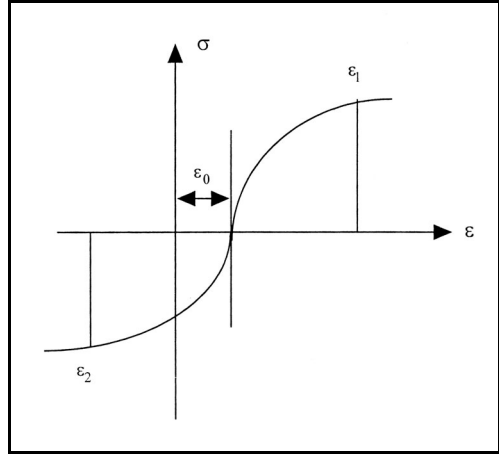


Figure 2. The shifted inelastic stress-strain diagram

$$P = -b \int_{-h_2}^{h_1} \sigma dy = -b \rho \int_{\varepsilon_2}^{\varepsilon_1} \sigma d\varepsilon = \frac{-bh}{\Delta} \int_{\varepsilon_2}^{\varepsilon_1} \sigma d\varepsilon \quad (6)$$

where $\Delta = \varepsilon_1 + \varepsilon_2$, b and h are the width and the depth of the section respectively.

The integral expression of equation (6) is equivalent to the area under the stress-strain diagram. Equation (6) provides a relationship between ε_1 and ε_2 for any given applied load.

The bending moment is given by the following relation:

$$M = b \int_{-h_2}^{h_1} \sigma y dy = b \rho^2 \int_{\varepsilon_2}^{\varepsilon_1} \sigma(\varepsilon - \varepsilon_0) d\varepsilon,$$

or

$$M = \frac{12I}{\rho \Delta} \int_{\varepsilon_2}^{\varepsilon_1} \sigma(\varepsilon - \varepsilon_0) d\varepsilon \quad (7)$$

where $I = \frac{bh^3}{12}$ is the moment of inertia for the section.

M can be derived for any set of values ε_1 and ε_2 . this is achieved by finding the static moment of the area under the stress strain diagram with respect to the centroid of the section.

M can be evaluated by performing the limited integration of Eq.(7) for any set of maximum stain values ε_1 and ε_2 .

3. MODEL DEVELOPMENT

For a given set of applied force P and bending moment M , equations (6) and (7) are the basic equations employed for the determination of the strain distribution across any section. The top and bottom strains are evaluated using the adopted bi-linear elastic stress-strain model shown in Figure 3. This idealized stress-strain model describes the material behavior in compression and tension.

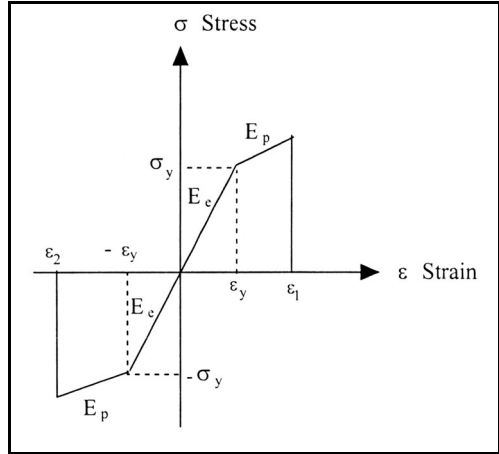


Figure 3. Bi-elastic approximation of the stress-strain relationship

Six different modes of strain can be identified in this stress-strain model. these strain modes are explained in the next section.

Modes of strain

The strain distribution across the section is assumed to be linear with an upper strain ϵ_1 and a lower strain ϵ_2 . Therefore, depending on the values of ϵ_1 and ϵ_2 in the above strain distribution, six different modes of strain can be identified. Three modes are in compression and the other three are in compression-tension states. These strain modes are described below:

Mode 1 Compression - elastic state, $|\epsilon_1| < \epsilon_y$ and $|\epsilon_2| < \epsilon_y$. the upper and lower strains are in compression and below the yield strain. The stress and strain distributions are shown in figure 4.

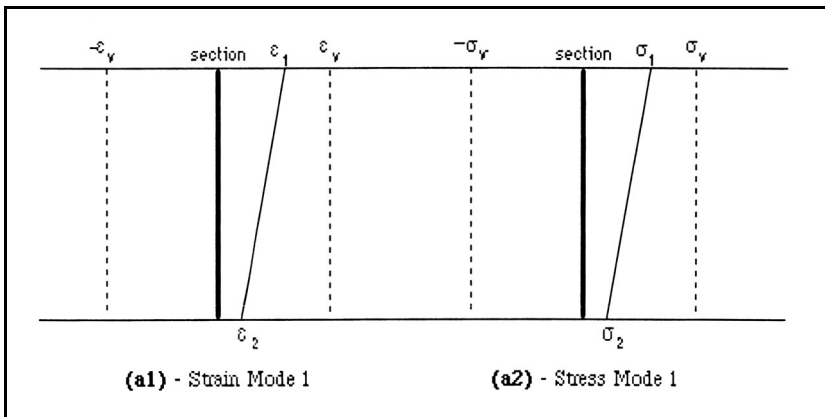


Figure 4. compression - elastic state

Mode 2 Compression - elastic/plastic state, $|\varepsilon_1| > \varepsilon_y$ and $|\varepsilon_2| < \varepsilon_y$. The upper compressive strain is plastic and the lower compressive strain is elastic.

Mode 3 Compression - plastic state $|\varepsilon_1| > 3\varepsilon_y$ and $|\varepsilon_2| > \varepsilon_y$. both upper and lower strains are in compression and exceed the yielding value.

Mode 4 Compression/tension - elastic state $|\varepsilon_1| < \varepsilon_y$ and $|\varepsilon_2| < \varepsilon_y$. the upper compressive strain is in tension and below the yield strain. The lower tensile strain is also below the yield strain. The section behaves elastically.

Mode 5 Compression/tension - plastic/elastic, $|\varepsilon_1| > \varepsilon_y$ and $|\varepsilon_2| < \varepsilon_y$. The upper compression strain exceeds the yield strain while the lower tensile strain is still below the yielding strain.

Mode 6 Compression/tension - plastic, $|\varepsilon_1| > \varepsilon_y$ and $|\varepsilon_2| > \varepsilon_y$. Both the upper compressive strain and the lower tensile strain exceed the yield strain.

Using the mathematical formulation of P and M discussed in the previous sections, a numerical model is developed to evaluate the upper and lower strains (ε_1 and ε_2) for any section starting from the knowledge of the loads applied. The technique implemented in evaluating ε_1 and ε_2 may be summarized as follows:

An initial set of values ε_1 and ε_2 is assumed. Based on these values, the axial force and bending moment are calculated. An iterative technique as shown in Figures 5 and 6, is employed to converge to a set of values for ε_1 and ε_2 for which the difference between the applied and the calculated forces is set below a preset tolerance. This technique is described by Terro and Hamoush (1996).

This iterative technique is implemented in the computer model to calculate the deflections and strains at each section from the knowledge of the axial force and the bending moment.

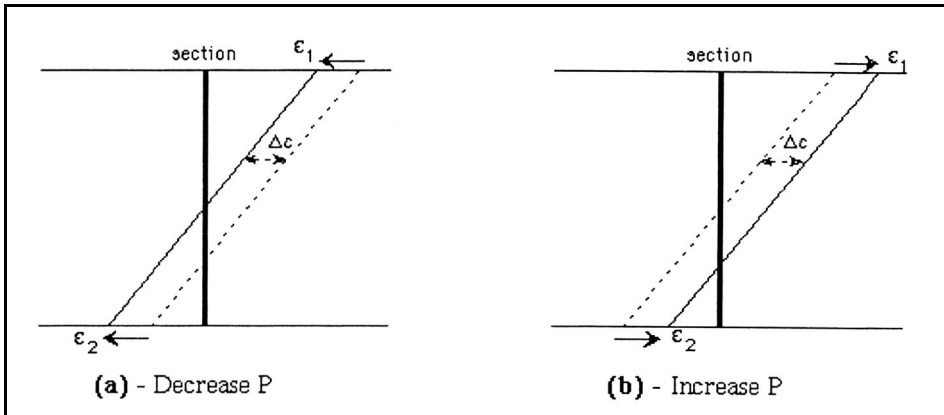


Figure 5. Correction of ε_1 & ε_2 to minimize ΔP

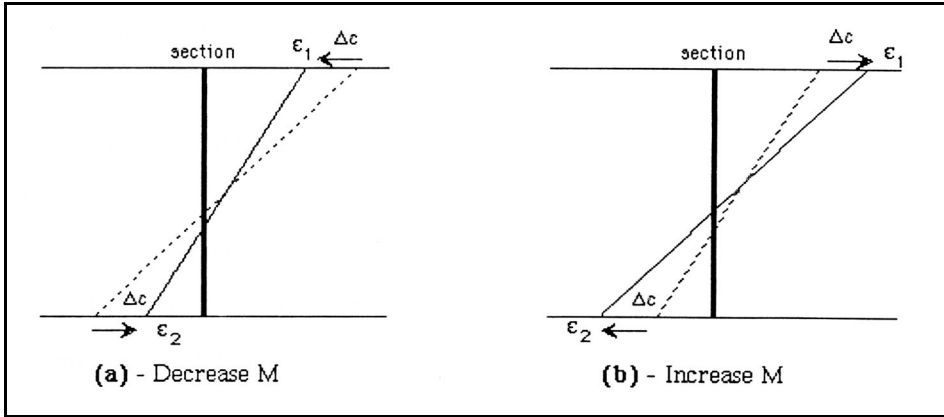


Figure 6. Correction of ϵ_1 & ϵ_2 to minimize ΔM

4. NUMERICAL APPLICATION

In this section, an example of a beam-column is analyzed using two cases of boundary conditions: simple supports and fixed supports. Different loading conditions are applied to both cases and the result obtained using the proposed model is validated against those derived from classical solution methods.

CASE A: Simply-supported symmetric beam

Figure 7 shows the discretization of a typical symmetrically tapered simple beam under combined axial and transverse loads.

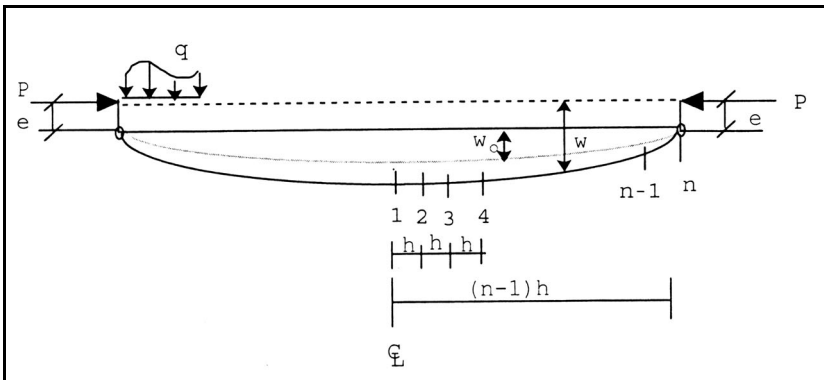


Figure 7. Finite Difference discretization of a symmetric simply-supported beam

The beam under study is linearly tapered and symmetric with respect to the mid-span. The cross-section at the ends is $279.4 \times 152.4\text{mm}$ (11×6 inches) while the middle section is $304.8 \times 152.4\text{mm}$ (12×6 inches). The elastic and plastic

moduli, E_e and E_p , are preset at 179.3 GPa (26000 ksi) and 17.93 GPa (2600 ksi) respectively. The beam has a length of 6.096m (20 feet) and is divided into 20 segments, 0.3048m (1 foot) long each.

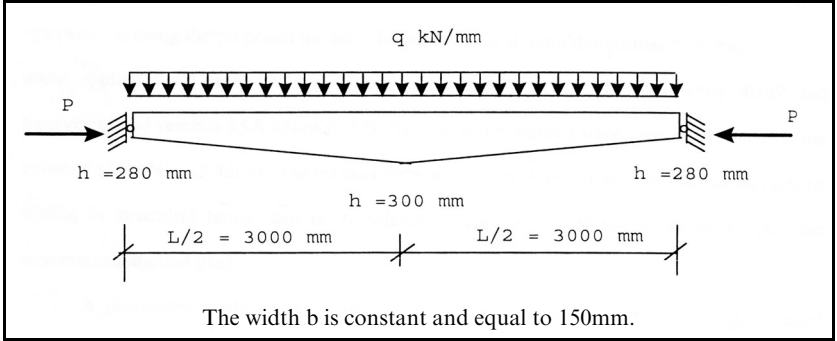


Figure 8. Simple beam used to verify the proposed model

The proposed numerical model is used to find the strain distribution and deflection at the cross section of each segment. An elastic finite element solution method (STAAD) is used for validation purposes. The beam is discretized into 20 two-noded beam finite elements with 21 nodes in total. Ranges of applied axial force, 10kN to 10,160 kN (2.25 kips to 2284.2 kips), and for transverse distributed loads, 5.3 kN/m to 73 kN/m (0.362k/ft to 5k/ft), are used in the analysis.

The mid-span deflection of the beam is compared to the elastic solution including $P - \delta$ effects. Table 1 shows a comparison between deflections obtained using the proposed model and the finite element method with 3 cycles and 9 cycles of $P - \delta$. The deflection results obtained using the proposed model coincide with those of the finite element method while the strain values remain in the elastic range. When the strains exceed the elastic range limit, the model yields higher deflection values.

Table 2 shows the upper and lower face strains together with the deflection of the midspan section using the proposed model. The behavior of the middle section becomes nonlinear when the applied axial force reaches 10,000 kN (2248.2kip) and the uniformly distributed transverse load reaches 55.8 kN/m (3.82k/ft). When the applied transverse loads exceeds the value of 55.8 kN/m (3.82k/ft), the method fails to converge to values of deflection and strains which, in structural terms, can be translated as the failure of the beam to support the incremented applied loads.

Table 1: The mid-span deflection of the beam analyzed using the proposed model, Staad with 3 cycles and 9 cycles of $P(\delta)$.

$\frac{q(\text{kN/m})}{P(\text{kN})}$	5.285	10.001	12.264	46.720	64.686	73.000	Model Used
10	1.392	2.692	2.997	11.811	16.002	18.009	Proposed Model
	1.372	2.642	2.946	10.922	15.464	17.805	STAAD 3 cycles
	1.930	2.794	3.150	12.319	16.761	19.050	STAAD 9 cycles
100	1.397	2.692	3.200	12.017	16.256	18.034	Proposed Model
	1.372	2.642	3.048	10.973	15.494	17.780	STAAD 3 cycles
	1.981	2.819	3.378	12.573	16.866	19.304	STAAD 9 cycles
1,000	1.422	2.769	3.429	12.573	17.018	19.050	Proposed Model
	1.387	2.743	3.327	11.735	15.748	18.542	STAAD 3 cycles
	2.007	2.921	3.607	13.208	17.043	18.796	STAAD 9 cycles
5,000	1.905	3.708	4.394	16.256	21.996	24.994	Proposed Model
	1.854	3.607	4.343	15.748	20.726	24.536	STAAD 3 cycles
	2.009	3.912	4.623	17.120	23.165	26.416	STAAD 9 cycles
10,000	3.099	5.994	7.188	31.496	Failed	Failed	Proposed Model
	3.048	5.842	7.112	28.552	38.659	43.510	STAAD 3 cycles
	3.266	6.325	7.569	30.894	41.834	47.092	STAAD 9 cycles

Table 2: The top and bottom strains, ε_1 & ε_2 , and the deflection obtained at the mid-span using the proposed model

$\frac{q(\text{kN/m})}{P(\text{kN})}$	5.285	10.001	12.264	46.720	64.686	73.000	
10	0.0610	0.120	0.130	0.520	0.700	0.790	$\varepsilon_1 * 10^{-3}$
	1.397	2.692	2.997	11.811	16.002	18.009	Mid-span defl. (mm)
100	-0.057	-0.110	-0.130	-0.520	-0.700	-0.780	$\varepsilon_2 * 10^{-3}$
	0.078	0.130	0.160	0.530	0.730	0.810	$\varepsilon_1 * 10^{-3}$
	1.397	2.692	3.200	12.014	16.256	18.034	Mid-span defl. (mm)
1,000	-0.041	0.092	-0.130	-0.500	-0.680	-0.770	$\varepsilon_2 * 10^{-3}$
	0.190	0.240	0.280	0.690	0.930	1.000	$\varepsilon_1 * 10^{-3}$
	1.422	2.769	3.429	12.573	17.018	19.050	Mid-span defl. (mm)
5,000	0.060	0.004	-0.014	-0.410	-0.550	-0.630	$\varepsilon_2 * 10^{-3}$
	0.700	0.780	0.810	1.260	1.700	1.800	$\varepsilon_1 * 10^{-3}$
	1.905	3.708	4.394	16.256	21.996	24.994	Mid-span defl. (mm)
10,000	0.530	0.460	0.430	0.129	-0.260	-0.350	$\varepsilon_2 * 10^{-3}$
	1.400	1.505	1.500	2.300	Structure	Structure	$\varepsilon_1 * 10^{-3}$
	3.099	5.994	7.188	31.496	Failed*	Failed*	Mid-span defl. (mm)
	1.100	0.970	0.920	0.094			$\varepsilon_2 * 10^{-3}$

* The failure of structure is determined when the bifurcation at mid-span occurs.

A parametric study of the beam-column example is performed for a range of axial forces and transverse loads and the deflection results are plotted in figure 9. The axial loads were varied within the range of 10 kN to 10,160 kN (2.25 k-2248.2k) and the transverse load in the range 5.3 kN/m to 73 kN/m (0.362k/ft-5k/ft). The plots in figure 9 represent the transverse loads versus mid-span deflection for each of the applied axial loads. The results obtained using the proposed model are compared to the finite element solution (STAAD) using linear assumptions. The deflections obtained by the proposed model were found to match with the finite element solutions when total behavior of all sections along the beam is elastic.

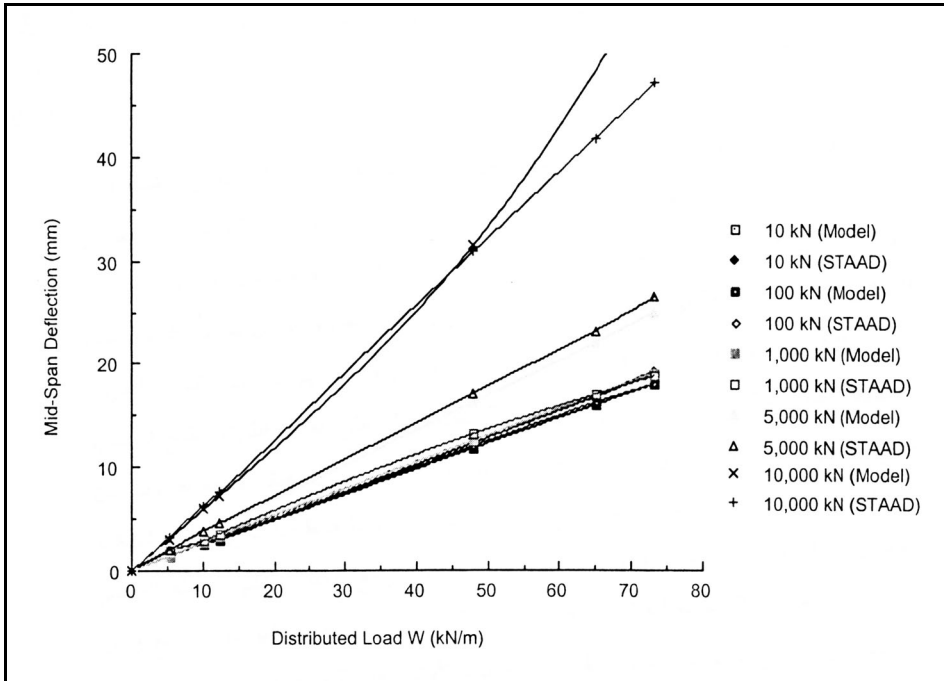


Figure 9. The mid-span deflections of the beam-column example under combined distributed and concentrated axial loads using the proposed model and STAAD (9 cycles).

When the strain in any section of the beam departs from the elastic range, the deflection obtained by the proposed model exceeds that of the linear finite element solution.

For the case when the transverse load is 65.4 kN/m (4.48 k/ft) and the axial force is 10,160 kN (2248.2 kips), the obtained deflection in the proposed model diverges at the point where $P = 10,160$ kN (2248.2 k) and $q = 55.8$ kN/m (3.821 k/ft). The strain in compression at the middle section exceeds the yield point and also the elastic deflection is under-estimated. When the axial force or

the transverse load exceeds the above limits, the beam becomes critical and failure by excessive deflection may occur.

CASE B: Symmetric beam with fixed supports

Figure 10 shows the discretization of a symmetrically tapered fixed beam under combined axial and transverse loads.

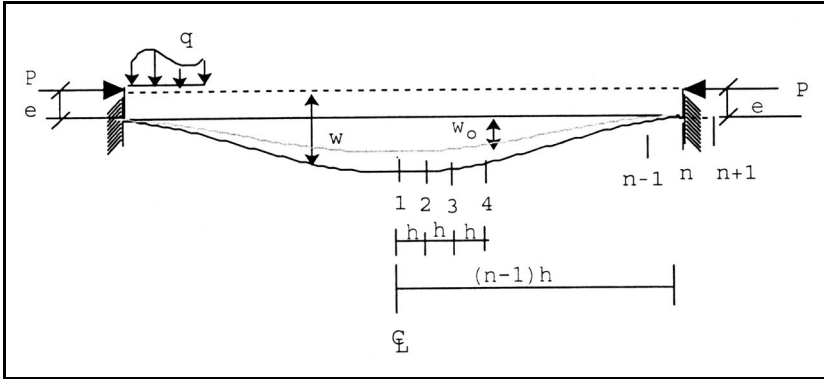


Figure 10. The Finite Difference discretization of a symmetric fixed beam

The beam-column example described in case A is analyzed with fixed ends boundary conditions. The applied axial force and the transverse load have the same limits as used for the simply supported case. Results summarized in Table 3 indicate that the beam remains in the elastic range. Table 3 shows the stations deflections and the elastic deflection using the finite element method. All strain and the deflection results coincided with those obtained using the finite element method including the $P - \delta$ effect.

Table 3. Mid-span deflections (in mm) of the fixed-beam under combined distributed q and axial load $P = 10,000$ kN.

q (kN/m)	Proposed Model	STAAD 3 Cycles	STAAD 9 Cycles
10.0	0.889	0.838	1.041
46.72	4.013	4.005	4.013
64.87	5.359	5.425	5.428
73.0	6.096	6.096	6.109

The top and bottom strains, ε_1 and ε_2 , at the ends of the beam are determined using the following relations:

- Form W''_n a relationship between ε_1 and ε_2 can be established as:

$$h = h_1 + h_2 - \rho(\varepsilon_1 - \varepsilon_2) \quad (8)$$

- Equilibrium of forces gives:

$$P = -b\rho \int_{\varepsilon_2}^{\varepsilon_1} \sigma d\varepsilon \quad (9)$$

Using equations (8) and (9), the strains ε_1 and ε_2 can be calculated.

- The equilibrium of moments, using the calculated values of ε_1 and ε_2 , gives a fixed moment as follows:

$$M = \frac{12I}{\rho\Delta} \int_{\varepsilon_2}^{\varepsilon_1} \sigma(\varepsilon - \varepsilon_0) d\varepsilon \quad (10)$$

5. CONCLUSIONS

The developed technique is based on establishing a moment-curvature relationship for sections subjected to a combined axial force and bending moment. Material and geometric non-linearity are considered in the method. Elastic-plastic constitutive relations are adopted to account for the material non-linearity. The geometric non-linearity is solved using a finite difference approach to predict the updated deflected shape of the beam-column in a step-by-step iteration procedure. This technique can be used to study non-prismatic beam-columns. Even though the investigation is carried out for beams with an axis of symmetry about the middle point, the model is capable of solving non-symmetric cases. A series of deflection values of nodes along the beam-column are obtained. These deflection values describe the final deflected shape of the element under study due to nonlinear behavior. The results from a number of cases were validated against those obtained from an established finite element structural program (STAAD). The method which was the subject of this research is accurate and fast compared to the finite element approach. This technique can be used to find the buckling behavior of the beam-columns which were under investigation by the authors.

REFERENCES

- Allen, H. G. and Bulson, P. S. 1980. Background to buckling, McGraw-Hill Book Company (UK) Limited, Maidenhead, Berkshire, England.
- El-Mezaini, N., Balkaya, C. and Citipitiogly, E. 1991. Analysis of frames with non prismatic members. Journal Structural Division ASCE 117(6): 1573-1592.

- Ferdis D. G. 1956.** Theoretical and experimental investigations on vibration susceptibilities of various highway bridges. Research report, Mich. Dept. Of Transportation, Lansing, Mich.
- Ferdis, D. G. 1966.** Dynamic hinge concept for beam vibrations. *Journal Structural Division ASCE* **92**: 1-8.
- Ferdis, D. G. 1973.** Dynamic and vibration of structures. John Wiley and Sons, Inc., New York, N.Y.
- Ferdis D. G. 1984.** Dynamics and vibration of structures. Revised edition., Robert E. Krieger Publishing Co. Malabor, Fla.
- Ferdis, D. G. and Keene, M. E. 1990.** Elastic and inelastic analysis of non-prismatic members. *Journal Structural Division ASCE* **116(2)**: 475-489.
- Ferdis, D. G. and Kozma, A. 1962.** Solution of deflection of variable thickness plates by the method of equivalent system. *Journal of Industrial Mathematics.* **12(1)**: 213-222.
- Ferdis, D. G. and Taneja, R. 1991.** Equivalent systems for inelastic analysis of prismatic and non prismatic members. *Journal Structural Division ASCE* **117(2)**: 473 - 488.
- Ferdis, D. G. and Zobel, E. 1958.** Equivalent system for the deflection of variable stiffness members. *Journal Structural Division ASCE* 123-129.
- Ferdis D. G. and Zobel E. 1961.** Transverse vibration theory, applications of equivalent systems. Roland Press Co., Inc. New York, N.Y.
- Funk, R. and Wang, K. T. 1988.** Stiffness of non prismatic member. *Journal Structural Division ASCE* **114(2)**: 484-496.
- Hamoush, S., Trovillion, J., Terro, M. J. and Shivakumar, K. 2001.** Design FRP Composites Materials For Upgrade of Concrete Frame Connections. CICI 2001-International Conference on FRP Composites in Civil Engineering Application, December 12-14, Hong Kong, China.
- Mumuni, I. 1983.** A finite element model for the analysis and optimal design of beams and plates with variable flexural rigidly. Thesis presented to Vanderbilt University at Nashville, Tenn in partial fulfillment of the requirement, for the degree of Doctor of Philosophy.
- Resende, J. W. and Doyle, B. J. 1981.** Non prismatic and effective non prismatic three dimensional beam finite element. *Computer and Structures* **41(1)**: 71-77.
- Shadid, Raza 1998.** Inelastic Analysis of Reinforced Concrete Beams Subjected to Combined Axial and Transverse Loads. A thesis submitted in partial fulfillment of the requirements for the degree of Master of Science, North Carolina A&T State University, USA.
- Terro, M. J. and Hamoush, S. A. 1996.** Inelastic analysis of sections subjected to axial force and bending moment. *Computer and Structures, An International Journal* **59(1)**: 13-19.
- Timoshenko, S. 1976.** Strength of materials. Part I; Elementary theory and problems, Third edition., Robert E. Krieger Publishing Co., Huntington, N.Y.
- Timoshenko, S. 1969.** Theory of elastic stability, Second edition. McGraw-Hill New York, N.Y.

Submitted : 6 December 2000

Revised : 2 January 2002

Accepted : 11 February 2002

التحليل المرن والغير مرن للأعضاء الغير منتظمة المقطع باستخدام الفروق المحددة

سمير حموش¹ و محمد ترو² و . و . مارك ماك - غينلي¹

¹ قسم الهندسة المعمارية - جامعة نورث كارولينا أ ت ستيت يونيفرستي - غرينزبورو
ن.س . 27411. الولايات المتحدة الأمريكية

² قسم الهندسة المدنية - جامعة الكويت - ص.ب . 5969 - الصفاة 13060 الكويت

خلاصة

يقدم هذا البحث دراسة عن السلوك المرن والغير المرن للأعضاء الغير ثابتة المقطع والمعرضة لقوى مركبة غير محورية وعرضية في نفس الوقت. وسلوك الأعضاء للمواد الغير مرنة تأخذ في الحسبان العلاقة الثنائية المرنة بين الأجساد والانفعال وهذا يحاكي التحليل المرن والغير مرن وهذا بالإضافة إلى التحليل الشامل من المرنة إلى اللدونة. وبذلك من الضروري جعل النموذج يتضمن مواد مختلفة مثل المعادن والخرسانة والمواد المركبة. وبناء على العلاقة بين التقوس والترخيم استخدم تقنيات الفروق المحددة لتحاكي شكل الترخيم للعناصر الغير منسوبة المقطع. وبناء على العلاقة الثابتة المقطع تم تطوير نموذج تحليل باستخدام الكمبيوتر لحالة الاتزان لمقاطع العنصر ليقدم حلول دقيقة لستة حالات من الانفعال: في حالة المرنة فقط وحالة المرنة مع اللدونة وحالة اللدونة فقط وذلك في حالي الضغط والشد ويربط النموذج بين التقوس للجسر والترخيم وذلك بتحليل توزيع الانفعال على مقاطع العنصر لعزوم الانحناء والقوى المحورية المعطاة. يعطي النموذج المقدم الحل لأي جسر غير ثابتة المقطع ولكن هذا البحث يركز على الكمرات المتناقصة فقط. وقد قدمت الأمثلة العديدة وحقق صحة ما تقدم على الحلول المرنة.